Spontaneous Unsteadiness and Sorting in Pyroclastic Density Currents and their Deposits

Peter Rowley[1], Rebecca Williams[2], Matthew Johnson[2], Thomas Johnston[2], Natasha Dowey[3], Daniel R. Parsons[4], Alison Provost[5], Olivier Roche[6], Gregory M. Smith[2], Nemi Walding[2]

Corresponding author: Pete Rowley. Email: pete.rowley@bristol.ac.uk

[1]School of Earth Sciences, University of Bristol, Bristol, UK
[2]School of Geography, Earth and Environmental Science, University of Hull, UK
[3]Department of the Natural and Built Environment, Sheffield Hallam University, Sheffield, UK
[4]Centre for Sustainable Transitions: Energy, Environment and Resilience, Loughborough University, Loughborough, UK
[5]Department of Earth Science and Engineering, Imperial College, London, UK
[6]Laboratoire Magmas et Volcans, University Clermont Auvergne, Clermont-Ferrand, France

This manuscript has not undergone peer review. It has been submitted for publication as a chapter within the AGU Special Publication "Particulate gravity currents in the Environment". Subsequent versions may have slightly different content. If accepted, the final version of this manuscript will be available via the "Peer reviewed publication DOI" link to the right on the website. We welcome comments or questions.

Spontaneous Unsteadiness and Sorting in Pyroclastic Density Currents and their Deposits

Peter Rowley[1], Rebecca Williams[2], Matthew Johnson[2], Thomas Johnston[2], Natasha Dowey[3], Daniel R. Parsons[4], Alison Provost[5], Olivier Roche[6], Gregory M. Smith[2], Nemi Walding[2]

[1]School of Earth Sciences, University of Bristol, Bristol, UK
[2]School of Geography, Earth and Environmental Science, University of Hull, UK
[3]Department of the Natural and Built Environment, Sheffield Hallam University, Sheffield, UK
[4]Centre for Sustainable Transitions: Energy, Environment and Resilience, Loughborough University, Loughborough, UK
[5]Department of Earth Science and Engineering, Imperial College, London, UK
[6]Laboratoire Magmas et Volcans, University Clermont Auvergne, Clermont-Ferrand, France

Abstract

Pyroclastic density currents (PDCs) pose substantial risk to populations living on and around active volcanoes, but their structure and internal dynamics are poorly understood. Much of this understanding is derived from interpretation of their widespread deposits. Scaled experiments are able to probe different conditions, to explore how changing flow dynamics relate to the wide variety of depositional styles observed in nature. Here we present two suites of work, first exploring the generation of spontaneous unsteadiness, and how it can impact the partitioning of sediment between dense granular under-currents, and over-riding dilute particle clouds. Second, we introduce grainsize variation to the dense granular regime and explore the formation of grading patterns. We demonstrate that unsteadiness in flow can be important in capturing different grading structures in deposits, and that granular sorting mechanisms are highly effective in thin fluidized grainflow. We conclude that this may raise challenges for the interpretation of common poorly sorted lithofacies (massive lapilli tuff) in natural deposits, as it must require substantial vertical mixing within these grainflows.

1 Introduction

Pyroclastic density currents (PDCs) are a widespread hazard at active volcanoes around the world, and understanding their internal dynamics remains a challenge to the volcanology community (Sulpizio et al., 2014; Lube et al., 2020). These currents can travel large distances from the volcano, at high speed, and pose considerable risk to communities living in volcanically active areas (Brown et al., 2017). PDCs are particle laden flows, comprising juvenile clasts, lithic fragments, and both

exsolving and entrained gases, are produced by a range of volcanic eruptive processes. They are thought to occupy a spectrum of behaviors, from very dilute turbulent currents to hyper-concentrated (dense) flowing mixtures, although there is little direct field data which helps address the question about the extent – both spatial and temporal – of these different conditions within different flows (Breard et al., 2016; Breard, Dufek and Roche, 2019). Moreover, it is also unknown how important these end-member flow conditions are in terms of relative transport capacity (Meruane et al., 2012; Breard et al., 2019; Lube et al., 2019; Smith et al., 2020), or the extent to which different regimes within a single current are, or are not, coupled to one another.

The deposits of PDCs are extremely varied, with lithofacies capturing a range of grainsize, sorting, fabric, and componentry relationships (Branney and Kokelaar, 2002). These lithofacies – and their horizontal and vertical relationships – have frequently been used to infer the behavior of the PDCs which have deposited them (Scarpati et al., 1993; Calder et al., 2000; Brown and Branney, 2004; Houghton et al., 2004; Giordano et al., 2010; Smith and Kokelaar, 2013; Douillet et al., 2019; Pollock et al., 2019; Cole et al., 2024), and how that behavior has evolved in time and space. The interpretation of these lithofacies, however, is based on assumptions about the flow conditions, based largely on drawing parallels from the hydrodynamic sedimentology literature, and insights from numerical and experimental modelling of granular currents. Grainsize variation has rarely been explored within the flowing dense granular regime, due to a range of complexities this introduces to modelling. Changes in the grainsize of a mixture result in changes in both the fluidization characteristics, and the pore pressure diffusion timescales (Gilbertson and Eames, 2003; Gilbertson, 2019), which result in mobility variation. Coupled with the particle segregation in agitated or flowing granular mixtures (Shinbrot and Muzzio, 1998; Khakhar et al., 1999; Shinbrot et al., 1999; Breu et al., 2003; Schnautz et al., 2005), exploration of diverse grainsize distributions comes with a number of poorly defined interactions which will likely impact the nature of deposition.

The key assumptions within much of the literature have not changed substantially since the widespread acceptance of the progressive aggradation paradigm (Branney and Kokelaar, 1997, 2002). That is, that the deposit from a current aggrades from the base of the over-riding current, and that vertical variation in the deposit is a result of a change in the type of material being supplied to the deposit through time. This is in contrast with the earlier "plug flow" paradigm in which the vertical structure of the deposit captures the vertical structure of the current, which comes to a halt to form said deposit. Within the present paradigm, then, a massive unit with inverse graded pumice clasts

would represent the deposit of a current which exhibited either a) deposition from a waxing current with increased transport capacity for larger clasts, b) a current with an increasing availability of pumice from eruption dynamic changes, c) local variation due to migrating thalwegs of flow, or d) floatation of large pumice clasts in very rapidly forming deposits (Branney and Kokelaar, 2002). These kinds of massive lapilli tuff (mLT) lithofacies are common within ignimbrite deposits, but no quantified process-product linkage has been definitively established to date.

Much of our understanding of PDCs comes from experimental modelling, which has used a wide variety of approaches and materials in order to explore different features and behaviors. The dense granular dominated regime has been explored using both short inertial (often dam-break) experiments, and more sustained long-lived supplies (Walker, 1981; Roche et al., 2004; Rowley et al., 2011; Smith et al., 2018; Gueugneau, Charbonnier and Roche, 2022). Dried, disaggregated natural PDC materials have been used in several experiments to observe the behaviors of pyroclastic charges (Girolami et al., 2010; Breard and Lube, 2017), although this leads to challenges in scaling, as particle sizes in the order of millimeters can be difficult to transport in laboratory scale flows, and the grainsize ranges in the laboratory are commonly narrower than those seen in natural deposits. As a result, many of these experiments have used analogue materials such as glass beads, particularly focusing on grainsizes between 45-90 microns. These small grainsizes allow pore pressures to develop, and for fluidization of the currents to occur, but are coarse enough that cohesive clumping is minimized and material handling is straightforward. However, these materials have grainsize ranges too large to become sufficiently airborne to generate any significant accompanying dilute current. In natural flows the smaller bulk grainsizes (fines down to <1 μm) and thicker flows (decimeter to meter scale) reduce pore pressure diffusion timescales, resulting in currents which – once fluidized – remain fluidized on the order of minutes or more.

The simultaneous existence of both a dense underflow, and a turbulent over-riding cloud has been well established in nature (Bursik and Woods, 1996; Branney and Kokelaar, 2002; Ort et al., 2003; Valentine et al., 2019), and described by the differing particle transfer mechanisms between layers (Doyle et al., 2010; Doronzo, 2012). Simultaneous dense and dilute flow behavior has only occasionally been captured experimentally (Dellino et al., 2007; Breard and Lube, 2017); laboratory work to date has typically focused on understanding the behaviors of only one part of this two-layer system (Dellino et al., 2010; Girolami et al., 2010; Andrews and Manga, 2012; Chedeville and Roche, 2014; Smith et al., 2018; Breard et al., 2019; Gueugneau, Charbonnier and Roche, 2022).

Evidence of flow unsteadiness is common in pyroclastic deposits (Branney and Kokelaar, 2002; Brown and Branney, 2004; Smith and Kokelaar, 2013; Douillet et al., 2019; Dellino et al., 2021), although the source of this unsteadiness is usually attributed solely to changing source parameters. Laboratory experiments are typically lock-gate release, and capture a short-lived single-pulse (waxing then waning) highly unsteady condition. However, experiments with sustained fluidization are able to capture the behavior of longer lived currents, and the formation of unsteadiness on timescales shorter than the waxing-waning of the bulk current (Rowley et al., 2014; Smith et al., 2018).

Unsteadiness has been observed in analogue models of the dilute regime and affects current structure, transport of particles and supply of material to the flow boundary zone (Andrews, 2019, Brosch & Lube 2020). Here we explore and build understanding of unsteadiness in coupled, two-layer flows through experiments in powder-grade fluidized materials. Given that in a two-layer current any sedimentation must pass through the dense undercurrent, and that the development of a flow boundary zone between loose substrate and shearing dense granular flow is assumed to be critical in the controlling the character of resulting deposits (Branney and Kokelaar, 2002; Zrelak et al., 2020; Smith et al., 2023), simulating the dense undercurrent itself is enough to understand the broad depositional behaviors of any PDC with a dense granular base. Assuming this, we investigate the signature of spontaneous unsteadiness in the propagation and deposition of dense granular currents, discuss the implications these observations have for the deposit sedimentology and stratigraphy, and explore the consequences of this new insight may have for the interpretation of natural PDC deposits. The application of polydisperse mixtures further enables us to look at the processes of sorting in dense granular flow and sedimentation, and to begin to evaluate some standing assumptions in the interpretation of natural deposits.

2 Methods

A total of 39 experiments were performed to execute this analysis (Table 1) using a range of different grainsize distributions. 10 different grainsize distributions were explored, using 5 different grainsizes (4-45, 45-90, 125-425, 425-600 and 600-800 μm). Between 2 and 5 repeats of each condition were conducted using varied camera placement during these repeats to allow investigation of different areas of interest with the high-speed camera. Overall behavior of each experiment type

was verified using wide angle oversight footage and final deposit comparison. Representative results from these runs are presented here to describe and characterize the behaviors of different materials. The flume is 150 mm wide, with a gas-permeable base through which an air supply can be provided, enabling the controlled fluidization and defluidization of the materials (Figure 1; the latter is a requirement for allowing deposits to develop).The gas supply is controlled to supply some fraction of the superficial vertical gas velocity at which intergranular friction is lost, known as the minimum fluidization velocity, Umf (Geldart, 1972; Gilbertson et al., 2008). Providing a gas supply below Umf allows deposition of material, and supplying at or above Umf keeps the material in a fluidized state. Material is released into the flume through the use of a raised hopper, with material release controlled by a simple sliding gate mechanism. The hopper opening is 65 cm above the base of the flume. Charges are well mixed prior to release, but we are unable to quantify any sorting processes which might occur between release and development of the flows observed here.

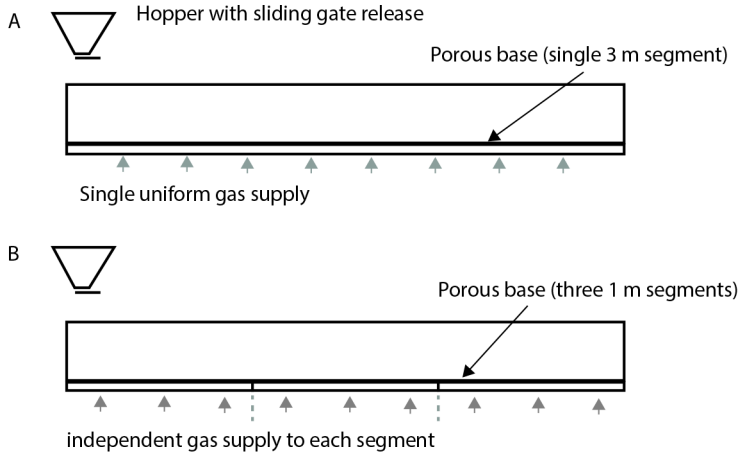

Figure 1 – experimental apparatus, highlighting the difference between the chambering of the gas supply through the porous base. A was used for the two-layer flow experiments, B was used for the deposition experiments.

Table 1 – Experimental mixtures

Experiment		% of each mix				
ID	Grainsizes	4-45 μm	45-90 μm	125-425 μm	425-600 μm	600-800 μm
A1	1	100				
A2	1	100				
A3	1	100				
B1	1		100			
B2	1		100			
B3	1		100			

B4	1	100			
B5	1	100			
C1	2	90	10		
C2	2	90	10		
C3	2	80		20	
C4	2	80		20	
C5	2	80		20	
D1	3	90	5	5	
D2	3	90	5	5	
D3	3	90	5	5	
D4	3	90	5	5	
D5	3	80	10	10	
D6	3	80	10	10	
D7	3	80	10	10	
D8	3	80	10	10	
D9	3	60	20	20	
D10	3	60	20	20	
D11	3	60	20	20	
D12	3	60	20	20	
D13	3	60	20	20	
E1	4	85	5	5	5
E2	4	85	5	5	5
E3	4	85	5	5	5
E4	4	85	5	5	5
E5	4	50	30	15	5
E6	4	50	30	15	5
E7	4	50	30	15	5
E8	4	50	30	15	5
E9	4	50	20	20	10
E10	4	50	20	20	10
E11	4	50	20	20	10
E12	4	50	20	20	10
E13	4	50	20	20	10

Two series of experiment are presented in this work; the first exploring the formation and behavior of coupled 2-layer systems using fine (4-45 μm) ballotini (experiments A1-A3), and the second exploring the sedimentary signature of unsteadiness in the dense undercurrent using coarser (45 – 800 μm) ballotini (monodisperse B1-B5, bidisperse C1-C5, tridisperse D1-D13 and quad-disperse E1-E13). All mixtures behave as Geldart Group A materials (Geldart, 1973). The larger grainsizes used in the second suite of experiments suppress the formation of a dilute layer, enabling a focus on the dense granular current, and exploration of sorting and sedimentation processes. All materials are heated to 70-80 °C overnight to remove moisture and minimize any moisture-related cohesion and clumping.

In both suites high-speed video was recorded through the flume sidewall perpendicular to the mean flow direction, at 500 frames per second to track flow behaviors (e.g. Flow speeds, thicknesses, etc.), the degree and nature of the unsteadiness within the current and the sequence of depositional processes and formation of the sedimentary structures and stratigraphies. The location of this camera was moved during different repeats of each condition in order to provide detail at various locations during the propagation and deposition. Secondary cameras were used to capture wide angle footage in order to verify similitude between repeats. In all cases flow front velocities were similar for each experimental condition, although the magnitude and timing of individual pulses in the current resulted in maximum runout varying within 150 mm of each repeat.

Scaling of these experiments follows established principles in similar works (Rowley et al., 2011; Roche, 2012; Smith et al., 2018). The parameters of the experiments and those of natural systems are defined – with their symbols - in Table 2. The dimensionless parameters in the lower part of Table 2 demonstrate that while the ranges of values in the experiments do not always match the ranges of natural conditions, they fall into the same behavioral types. The only substantial scaling issue would appear to be the more rapid defluidization experienced by the laboratory flows, which – in these experiments – is countered by the constant supply of fresh gas to the base of the current.

2.1 Two-layer flow experiments

Experimental currents were generated using 10 kg of heated (70°C) silica beads with diameters between 4- 45 μm. These were fed from a hopper with a fixed mass flux of 2.5 kg/s (confirmed by logging mass balance, Rowley et al 2014), into a 3 m long 150 mm wide horizontal flume, in which a sustained gas supply was fed through a single uniform porous base for the duration of the experiments.

2.2 Deposits from polymict granular flow

Experiments in this suite were similar to those in the previous suite, but used a flume in which the first 1 m of runout was supplied with a basal gas flux in excess of the calculated Umf for each mixture, and the rest of the 3 m flume supplied with ~80% Umf to enable a deposit to aggrade.

Table 2. Parameters of natural dense PDCs compared with the experimental currents in this work.

Parameter	Dense PDCs *	2-layer experiments (dense layer)	Deposition experiments	Significance

Particle Diameter (m)	$2x10^{-5} – 5x10^{-4}$*	$4.5x10^{-5} – 2.5x10^{-4}$	$4.5x10^{-5} – 2.5x10^{-4}$	
Particle Density (kgm^{-3})	500-2500	2500	2500	
Particle Volume Fraction φ_s	0.3-0.6	0.6	0.6	
Fluid Density (kgm^{-3})	~1	1.225	1.225	
Fluid Viscosity ($kgm^{-1}s^{-1}$) μ	$\sim10^{-5}$	$1.78x10^{-5}$	$1.78x10^{-5}$	
Hydraulic permeability	$10^{-12} – 10^{-10}$	$2x10^{-14}$ - $2x10^{-12}$	$2x10^{-12}$ - $8x10^{-10}$	
Hydraulic diffusion coefficient	$10^{-4} – 10^{2}$	$10^{-4} – 10^{-2}$	10^{-2}-10^{1}	
Acceleration due to Gravity (ms^{-1})	9.81	9.81	9.81	
Flow Thickness (m) H	$10^{0} – 5x10^{1}$	$1x10^{-4} – 5x10^{-3}$	$1x10^{-4} – 5x10^{-3}$	
Flow Length (m)	10^{3}-10^{4}	0.5-3	0.5-3	
Flow Front Velocity (ms^{-1}) U	5-30	1.5 – 2.5	1.5 – 2.5	
Slope Angle (°)	0-30	0-5†	0-5†	
Dimensionless parameters				
Fluidization number (N_F) **	$10^{-7} – 10^{-3}$	$10^{-5} – 10^{-4}$	10^{-3} - 10^{0}	Flow velocity much greater than fluidization velocity
Bagnold Number (N_B) †	10^{0}-10^{2}	10^{-2} - 10^{0}	$10^{0} – 10^{2}$	Macroviscous to intermediate
Savage Number (N_S) ‡	$10^{-9} – 10^{-8}$	$3x10^{-11} – 3x10^{-2}$	$3x10^{-11} – 3x10^{-2}$	Frictional
Froude Number (Fr) [a]	1.6-3	2-20	2 - 20	Supercritical
Darcy number (N_D) [b]	10^{1}-10^{4}	10^{-1} - 10^{1}	10^{-1} - 10^{1}	Solid-fluid interactions dominate
Mass number [c]	10^{2} - 10^{3}	10^{3}	10^{3}	
Pore pressure number (N_P) [d]	10^{-4}-10^{1}	10^{-1}-10^{-2}	10^{0} - 10^{1}	Pore pressure diffuses more rapidly in experiments
Stokes number (St) [e]	10^{-5} - 10^{3}	$10^{-3} – 10^{-1}$ *10^{-3} f*	$10^{-1} – 10^{2}$	Efficient coupling of particles to gas in fine materials. Poor coupling in course. Dilute layer is well coupled.

* (Roche, 2012; Fries, Roche and Carazzo, 2021)

** Ratio of interstitial gas velocity over the flow velocity (Denlinger and Iverson, 2001)

† Ratio of collisional over viscous stresses (Bagnold, R. A., 1954)

‡ Ratio of collisional over frictional solid stresses when pore fluid pressure is negligible. (Savage and Hutter, 1991)

[a] Ratio of inertial stresses over viscous stresses

[b] Ratio of viscous solid-fluid interactions over collisional stresses (Denlinger and Iverson, 2001)

[c] Ratio of solid over fluid inertia (Iverson, 1997)

[d] Ratio of pore pressure advection timescale over the pore pressure diffusion timescale (Denlinger and Iverson, 2001)

[e] Ratio of particle response time to timescale of flow (Israel and Rosner, 1982)

[f] Stokes number calculated for the dilute layer assuming 1% particle concentration

3 Results

3.1 Two-layer flow unsteadiness

On reaching the channel base, the powder spontaneously partitioned into a two-layer current, with limited but non-zero coupling between them (Figure 2). The initial part of the charge, which was interacting with an empty flume base was largely lofted into forming a dilute flow, by energetic impingement. Some of this material followed ballistic trajectories to rain back to the flume base. Much, however, remained lofted and entrained in the air, developing a dilute cloud which was observed to flow away from the impingement area. This dilute layer demonstrates good coupling to the carrier gas (St ~10-3, Table 2). Over the following seconds this dilute layer developed turbulent structures, and a concentration profile as indicated by the albedo of the layer – higher particle concentrations are in evidence closer to the flow base. We have not been able to quantitatively calibrate albedo to concentration in these experiments.

A dense underflow was also observed to form almost immediately after the first particles develop the dilute cloud. This dense current is formed by material arriving from the hopper onto a flume base which already has material on it, and by the raining out of sediment from the dilute flow above into the basal region of the flume. This dense current grows from a few millimeters thick to several centimeters as the experiment progresses. The dense flow develops unsteady pulses within the first 0.3 seconds, which last for the duration of the experiment. The pulses are characterized by regions of the dense current which are approximately 2-3 times the thickness of the thinnest parts. These wave-like surface morphologies are observed to become sequentially bigger, such that those entering the flume in the first 0.4 seconds are up to 30 mm high, while those after a second are in the order of 50-60 mm high. The thinnest parts of the dense currents are observed to grow from approximately 5 mm in the first second, to 20-30 mm after 2 seconds. As the experiment progresses, these surface waves take on steeper bore-like forms, and are eventually observed to form breaking wave type structures within the flow, often throwing material from the dense current into the turbulent suspension above.

The interface between the two flow layers is observed to be sharp and distinct. Fallout sedimentation from the dilute layer feeds material into the dense current, while unsteadiness in the dense layer was important in supplying the dilute layer as sloshing and breaking-wave events intermittently threw material into the dilute layer. This instability in the dilute sediment load was concentrated between 2-4 seconds of the current entering the flume, and correlates to the period of highest breaking wave activity in the dense flow. The resulting temporally and spatially variable mass in both layers was chaotic, and resulted in pulses of high and low concentration in the dilute flow passing through the flume, which persisted across the length of the flume.

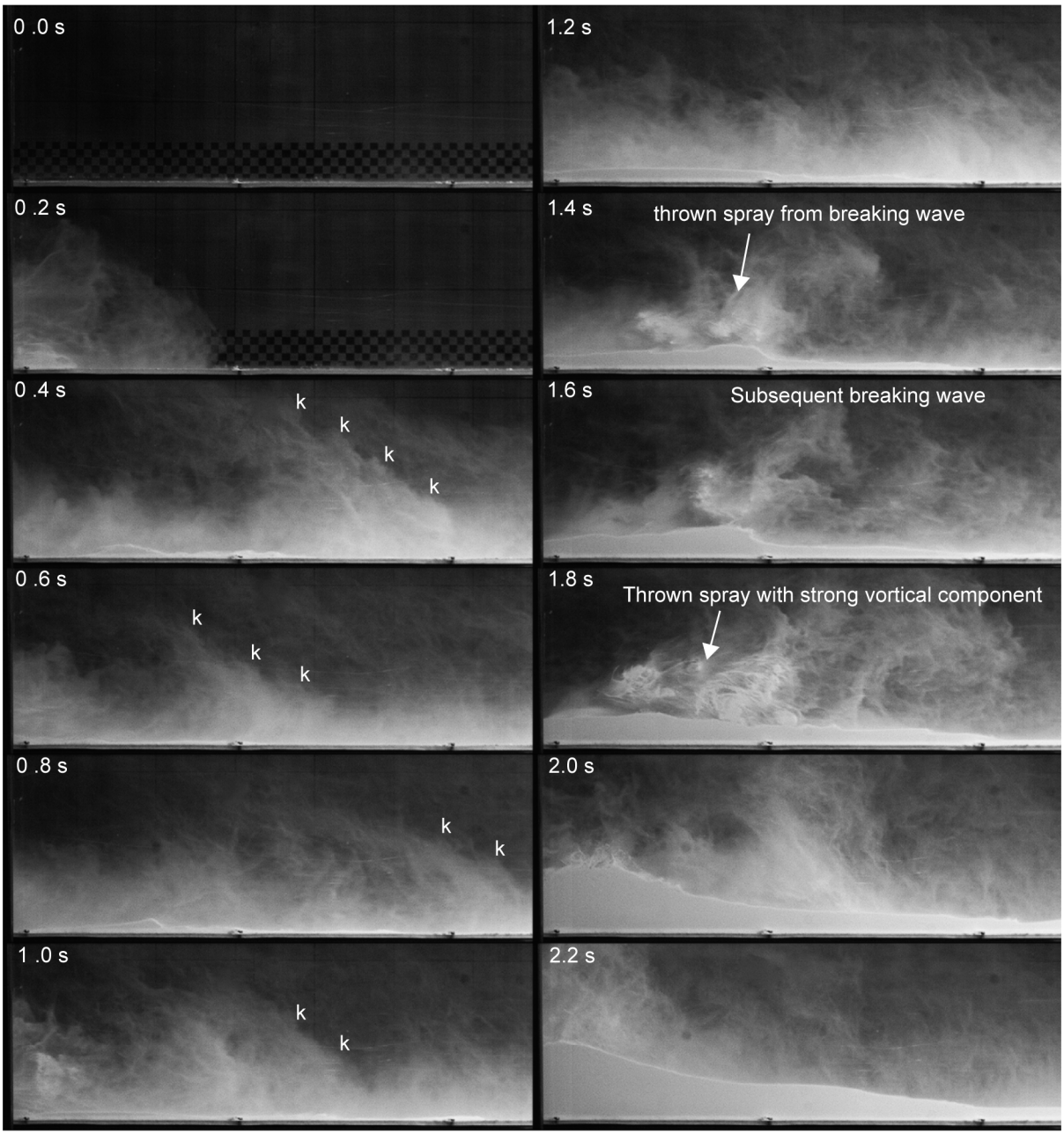

Figure 2 High speed video sequence showing passage of a 2-layer current (Experiment A2, Table 1). Dilute layer arrives first, followed by a thin dense layer exhibiting extreme unsteadiness. Flow pulses up to 3 cm thick surge ahead of layers less than 1 cm thick. Both the dense and dilute layers have bulk velocities in the order of 2 m/s. Large energetic pulses in the dense layer result in spraying of material into the over-riding dilute layer, and sediment rains from the dilute layer into the dense. By 1.6 s into the current a deposit is beginning to form, which suppresses the passage of air to the free surface, further decelerating the current and causing thickening of the deposit. Turbulent structures are evident in the dilute flow by 0.4 seconds, including cm-scale Kelvin-Helmholtz instabilities on the larger rolls (labelled k), mirroring those observed in other dilute flow experiments (Andrews and Manga, 2012).

Pixel brightness can be used as a proxy for sediment concentration in the turbulent suspension (e.g. Andrews & Manga 2012). While we are unable to correlate brightness values to specific concentration, we can conduct a relative comparison to view the development of unsteadiness in the dilute cloud. For the analysis the pixel column at the right edge (flume exit) was analyzed at 0.1 second intervals, to capture the broad evolution of the sediment concentration throughout the experiment. The mean brightness of this column captures the variation in flux of material in the dilute column (Figure 3A). The vertical variation can be seen in the composite image of these edge slices which are compiled to provide a temporal evolution of the flume exit (Figure 3B). The mean pixel values were calculated from only the dilute portion of the data; the dense current can be seen in these edge pixels from about 1.5s into the experiment, and these were excluded from the calculations.

The head and body of the dilute layer maintained a velocity of 2.2 +/- 0.2 m/s for the duration of the experiments. The dense layer propagates at 2.1 +/- 0.3 m/s, although these velocities can only be made by tracking the front of the current and surface features of the layer controlled by pulses of material. Based on the observations at the flume exit (Figure 3B) and the observed velocities, the eddies in the dilute layer – as shown by periods of high sediment concentration at the exit – have passage durations in the order of 0.1 – 0.4 seconds, which correspond to a turbulent length scales in the order of 0.2 - 0.8 m.

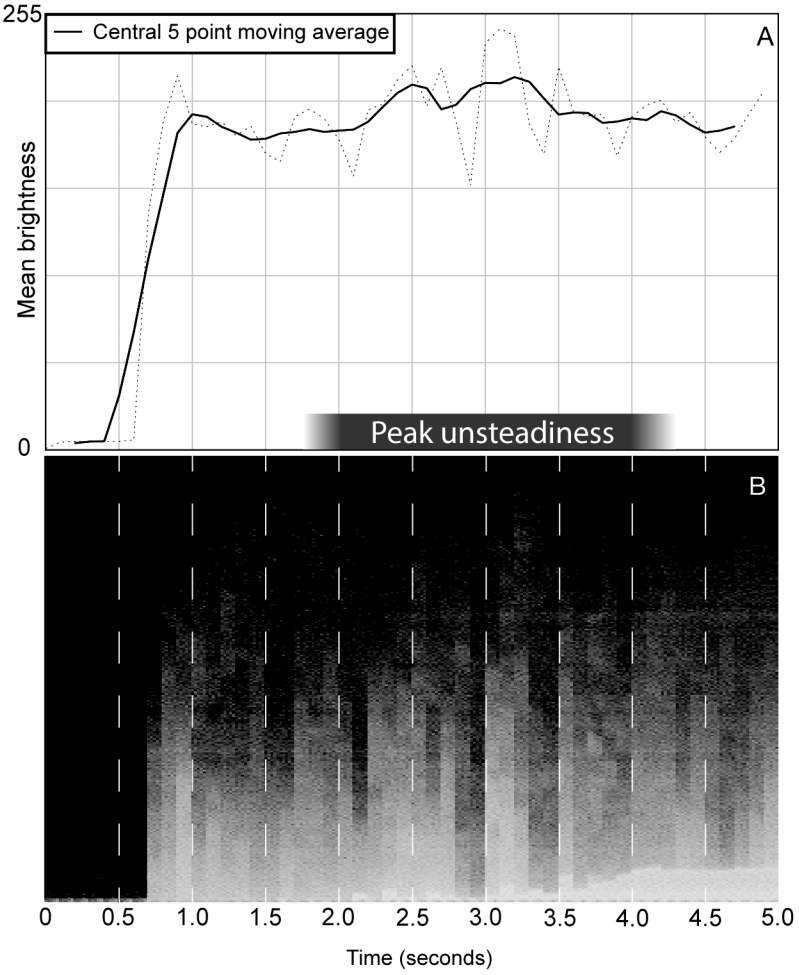

Figure 3 A - Time-series mean brightness plot for the distal-edge pixel column in the frame. The dark black line is a 5-point moving average, demonstrating elevated brightness (sediment load) during the unsteady wave-dominated phase. A peak in brightness in the dilute layer is observed during the peak sloshing and breaking-wave activity in the dense layer (2-4 sec, labelled "peak unsteadiness"), indicating an increase in sediment transferred to the turbulent suspension. B – time-series of the distal-edge pixels at 0.1 second intervals through the experiment. This demonstrates unsteadiness and vertical heterogeneity in sediment load complimentary to (A), as well as deposit and underflow growth through time at that location.

3.2 Deposition from a polymict dense granular layer

Moving to experiments using coarser (45-90 μm) ballotini allows us to investigate the behavior of the dense layer without the complexity of fines lofting above it. Several works have explored the

formation of deposits for fluidized and aerated dense granular currents, and the generation of bedforms within them (Rowley et al., 2014, 2023; Smith et al., 2018, 2020). Here we add a range of grainsizes to the bulk charge to explore the formation of sorting profiles in dense granular currents and explore their resultant deposits. In particular, we are able to observe how these sorting behaviors express themselves when unsteadiness appears within the currents in the form of flow pulses and stepwise aggradation of a deposit (Sulpizio and Dellino, 2008). The structure of the deposits produced in these rapidly fluidizing experiments is not meant to be directly analogous to the architecture of PDCs, but enables us to explore different sedimentary behaviors and characteristics at a range of bed angles and flow conditions (Figure 4).

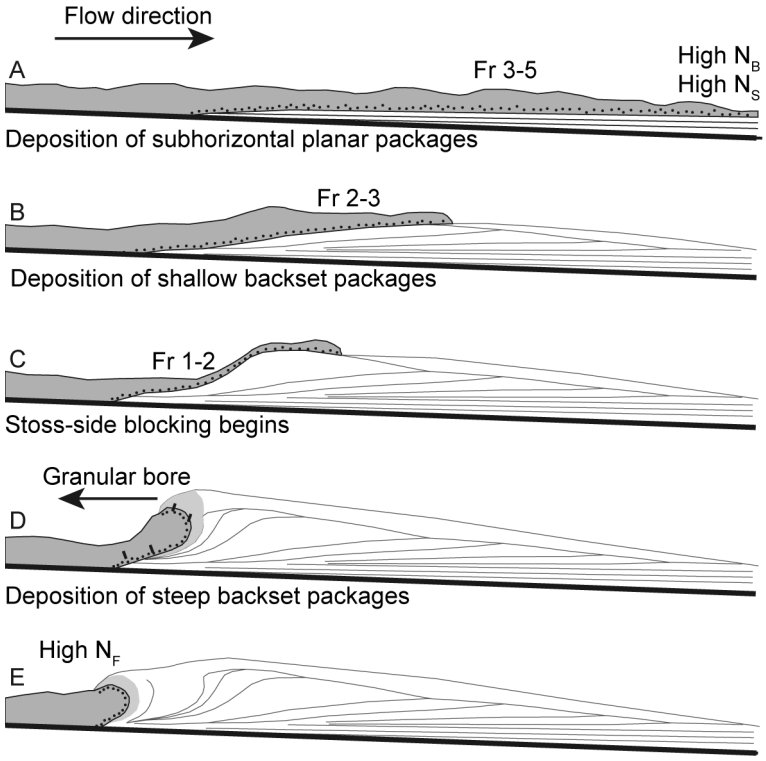

Figure 4 – Process of bedform development in laboratory experiments of fluidized dense granular currents (modified from Smith et al 2020).

Currents are described using the dimensionless Froude number (Fr), Bagnold number (NB), Friction number (NF) and Savage number (NS), and particular bed sets are related to specific conditions in the current (Smith et al 2020). Planar beds are found to occur during low slope angle propagation

when currents exhibit high Bagnold numbers, and Savage numbers in the higher collision dominated rather than contact shearing dominated regime (Zhou et al., 2016) (NS>0.1 and NB>450). Backset bedforms occur as the current interreacts with steeper slopes, with higher frictional stresses, and the current moves from supercritical to critical Froude numbers. At this point the current is observed to become blocked behind the existing deposit, builds a large volume of fluidized material of approximately the deposit height, before cascading back up the flume as a granular bore. The upstream growth of the deposit is captured as rapidly deposited very steep (>angle of repose) bedform cross-sets, before the bore collapses and the cycle is able to repeat itself. Throughout this process the deposit is aggraded via a stepwise process, where sets that are 5-50 mm thick are set in place, preserving the vertical structure of the current from which they formed. This stepwise aggradation process is in contrast to the traditional plug flow and more widely accepted progressive aggradation models usually discussed in terms of PDC deposit accumulation (Branney and Kokelaar, 2002; Sulpizio and Dellino, 2008).

In these dense flow experiments we see the same spontaneous unsteadiness, and resulting surface waves which were observed in the previous 2-layer currents (Figure 5a). Previous work in similar materials noted that stepwise aggradation was a feature of supercritical (Fr~7) pulses coming to a halt, and that flow unsteadiness increased as the current became less aerated (Smith et al., 2018). More significantly however, when polydisperse mixtures are used, these unsteady pulses and waves become involved in particle sorting processes (Figure 5b&c). The sorting occurs rapidly within the current, with well-defined coarse and fines enriched layers present after just 10-20 cm of transport. Larger particles (>400 μm) travel at the top of the current, with both large and small particles coupled to the bulk current speed. Currents travel at 1.7 +/- 0.3 m/s as they encounter the defluidizing section of the flume, and noticeable sorting is occurring in the first 0.1 seconds of flow. Assuming an average current thicknesses on the order of 1 cm equates to vertical particle velocities in the order of 0.1 m/s.

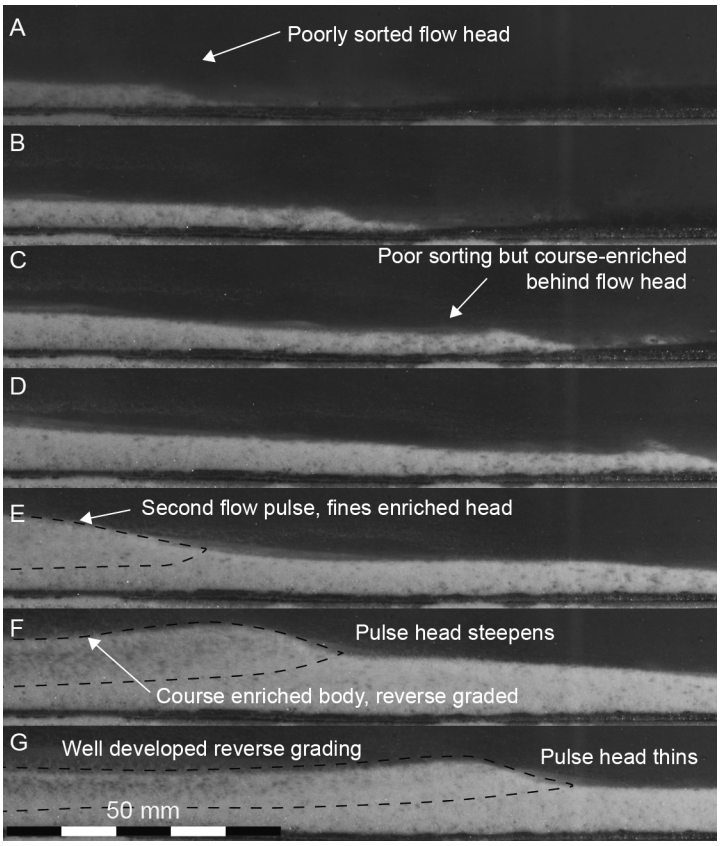

Figure 5 - High speed video frames at 0.03 second intervals from experiment 3 (Table 1) containing 90% 45-90 micron ballotini, and 10% 125-355 micron ballotini. Following the passage of a poorly sorted current head, unsteady pulses of material transport graded currents, which have sorted before entry into frame (50 cm downstream of hopper).

The confluence of sorting processes within the current, and stepwise aggradation of the deposit results in a complex deposit stratigraphy, with a range of grading patterns (Figures 6 & 7). Low angle beds deposited through sequential deposition of course-enriched flow heads, and fines-enriched bodies results in normal grading at the distal end of the deposit, while 'freezing' of vertically sorted forward-propagating pulses creates reverse grading profiles in the mid section. As the steeper backsets begin to develop at the proximal end the sorting relationships change, revealing either a poorly sorted mixing, or reorganization to normal grading of particles.

3.3 Sorting processes

The accumulation of reverse graded packages from individual current pulses is demonstrated in Figure 7. A new current pulse arrives to the deposit, stalls at the adverse slope, preserving the

granular sorting which has occurred during flow. Once this package comes to rest, a new current package begins propagating across its free surface for the cycle to repeat again. In this way many reverse graded packages of cross stratified sets accumulate within a single deposit, each package the result of an individual unsteady pulse.

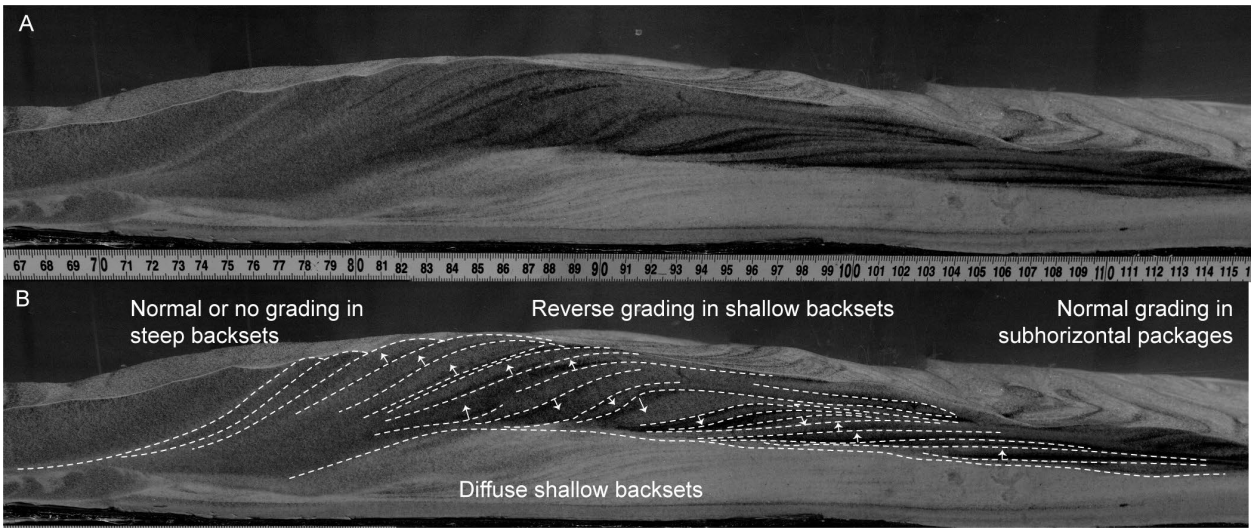

Figure 6 A - Profile of deposit from experiment E5 (Table 1) with B - annotations delineating grading patterns observed in the deposits. Arrows indicate fining direction (i.e. upward arrows are normally graded, downward arrows are reverse graded).

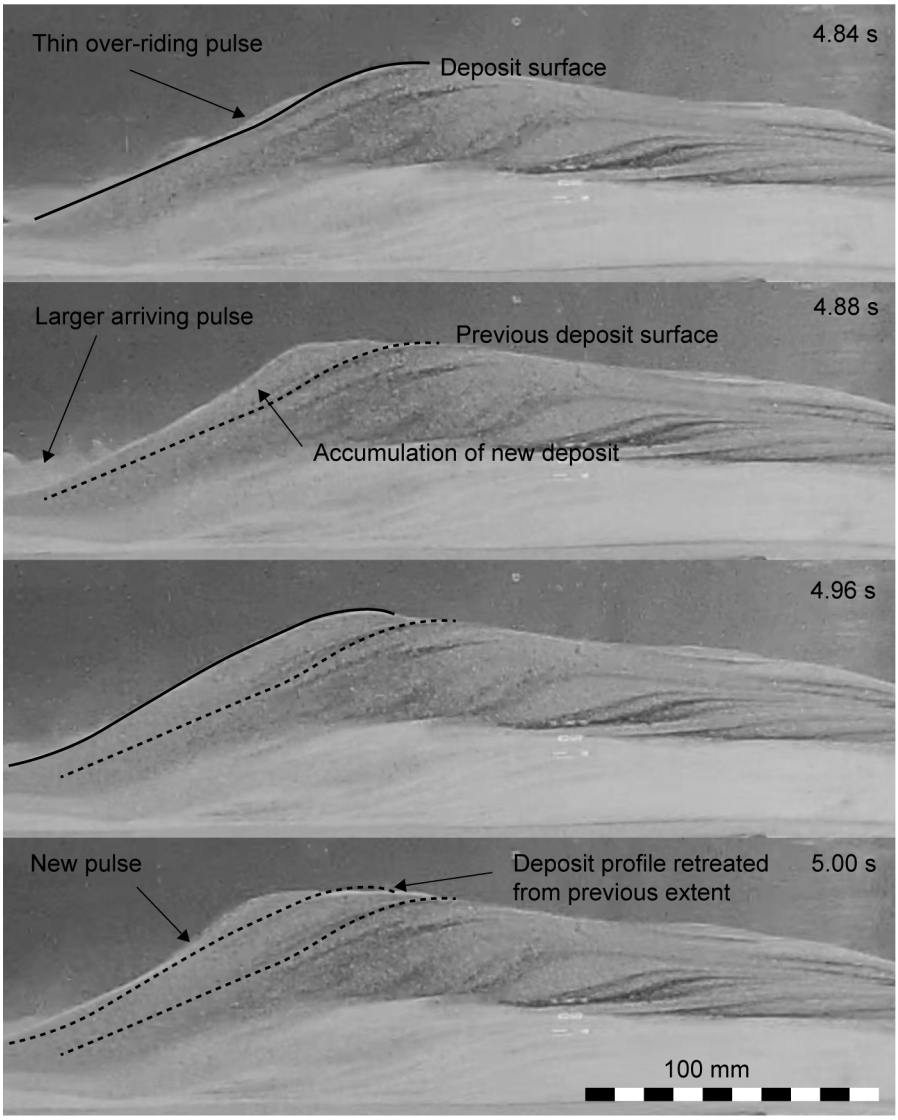

Figure 7 - Video frames from experimental current showing an aggrading deposit from a stratified current, current head enters the frame at 4.84 seconds. By 4.96 seconds a new graded bed has formed, and a new pulse begins to form a new package. Between 4.96 and 5.00 seconds there has been some minor (3-5 mm) loss of material at the top of the first package, suggesting slight slumping back of this layer as it settles.

The nature of the grading process can be captured using image analysis to explore the grainsize parameters for a given package. In Figure 8, a single package of the deposit from a 4-component current (comprising 45-90 micron, 125-425, 425-600, and 600-800 micron particles, experiment E5, Table 1). The package is divided into 5 equal stratigraphic horizons, with 200 randomly selected

particle measurements (longest axis) taken within each package. We see a systematic change in grainsize distribution throughout each of the sets, with a reduction in relative fines and increase in relative coarse material higher in the deposit. This correlates to a change in sorting index from relatively well sorted to poorly sorted during deposition.

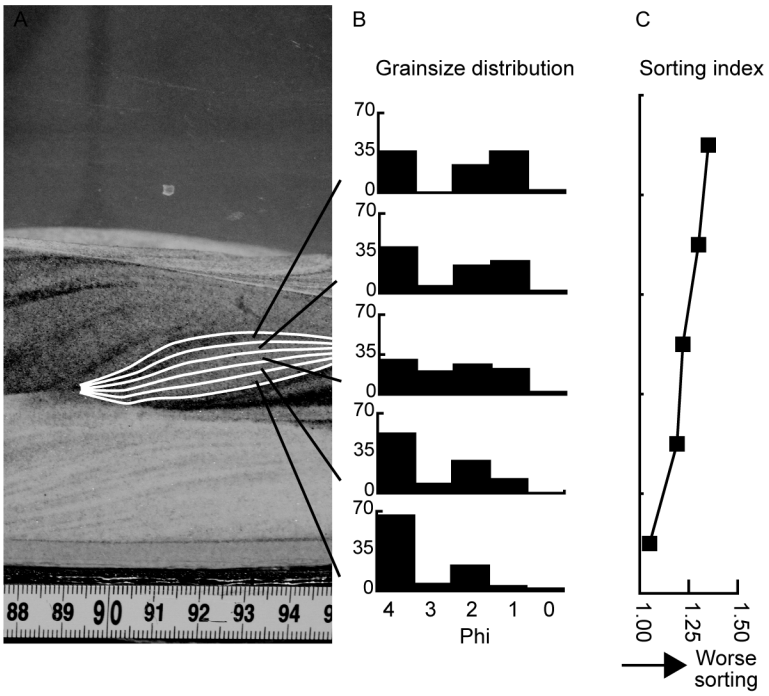

Figure 8 – Sorting characteristics through a single deposit package in a polydisperse (4 grainsize) experiment, showing inverse grading with progressively better sorting characteristics toward the top of the package.

The nature of the grading process can be captured using image analysis to explore the grainsize parameters for a given package. In Figure 8, a single package of the deposit from a 4-component current (comprising 45-90 micron, 125-425, 425-600, and 600-800 micron particles, experiment E5, Table 1). The package is divided into 5 equal stratigraphic horizons, with 200 randomly selected particle measurements (longest axis) taken within each package. We see a systematic change in grainsize distribution throughout each of the sets, with a reduction in relative fines and increase in relative coarse material higher in the deposit. This correlates to a change in sorting index from relatively well sorted to poorly sorted during deposition.

4 Implications for mobility

Spontaneous unsteadiness appears to be an inherent characteristic of dense granular currents, and we can anticipate that this holds true for the dense undercurrent in stratified PDCs. The temporal and spatial variation in energy flux can therefore be expected to be important in controlling localized depositional and erosional processes. The vast array of stratigraphic relationships seen in PDC deposits in the field may be subject to modification by, if not a direct result of, such unsteadiness.

Sorting behaviors within currents raise a series of interesting questions regarding the propagation and mobility of dense granular layers. In particular, the relationship between grainsize and fluidization is well known, and mixtures with fine particles are known to be much more able to fluidize, with lower gas escape velocities than coarser mixtures with limited fines. This implies that in a size-stratified current (e.g. Figure 5), the underlying fines-enriched material will be more mobile than the coarser upper layers. This assumes that other behaviors not observed in these experiments such as elutriation of fines do not overwhelm the kinetic sorting processes.

5 The massive lapilli tuff question

Formation of massive lapilli tuff (mLT) is argued to capture the sedimentation by progressive aggradation from the dense layer within PDCs (Branney and Kokelaar, 2002). The vertical and lateral variation of these deposits is seen as a record of variations in the current as it evolves due to changing eruption conditions and local topography/environment through space and time. The generally poor sorting which characterizes mLT is, however, problematic for the deposition by progressive aggradation from any current which resembles those we see in the laboratory.

Progressive aggradation requires the vertical migration of the flow boundary zone, such that the deposit captures the particle distribution within the current without substantial tractional shear sorting processes happening. However, The flow boundary zone typically has considerable shear (Breard et al., 2016; Breard and Lube, 2017; Smith et al., 2023). Therefore, the vertical migration must act rapidly, but, more importantly, must be capturing a poorly sorted granular mixture. This rapid shearing observed under a range of experimental conditions is in contrast to the imagined shear profiles originally proposed for progressive aggradation of mLT (Branney and Kokelaar, 2002).

The results presented here demonstrate that thin laminar granular flow, even with considerable spatio-temporal unsteadiness, is able to quickly and efficiently develop sorting profiles. Such a current would be unable to deposit mLT without depositing much coarser units further downstream. This is not typically observed in the field - although can be the case for small volume unsteady PDCs, where lenses enriched in block-size clasts reach distal extents (Lube et al., 2007). We therefore conclude that in PDCs which deposit mLT, there must be some considerable vertical mixing which occurs on a larger scale than the granular temperature fluctuations driving the sorting processes, as seen here in the unsorted steep backsets where granular bores interact with forward-propagating pulses to develop strong mixing conditions. We postulate that for mLT to be deposited the dense granular regime requires two distinct elements; a thin flow boundary zone which migrates vertically with aggradation, and an upper – poorly sorted and vigorously mixed dense granular current which is fed into the upward migrating flow boundary zone (Figure 9). The vertical aggradation rate would need to be sufficiently rapid to suppress development of shear-related sedimentary structures, and the thinner the flow boundary zone the less effective the current will be at stripping large particles from the aggrading bed.

The unsteady pulses which develop in the currents observed here are not just surface features, but have a penetration depth into the preceding body of current (Figure 5). We therefore suggest that this may impose the necessary energy to cause the mixing required. Mixing in this upper layer would be likely to be reinforced by (or even a driver of) the surface waves which have been observed in the laboratory seen here and in previous work (Rowley et al. 2023).

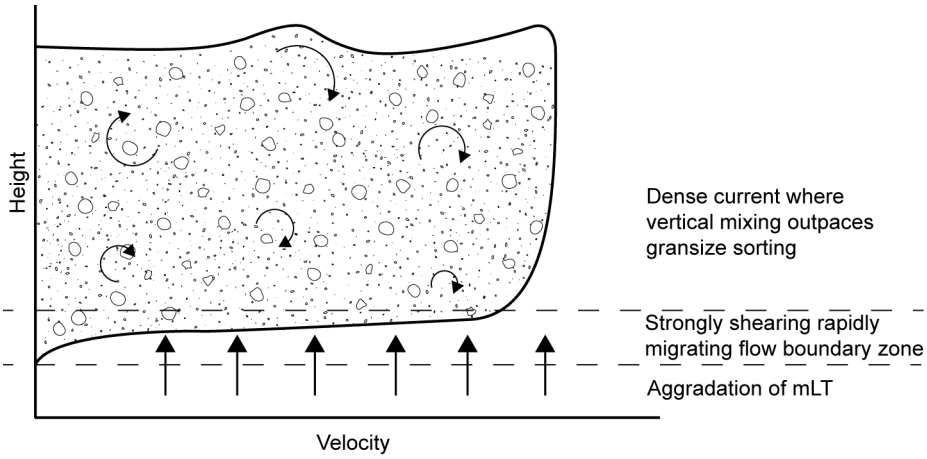

Figure 9 – Model of mLT aggradation where rapid migration of the flow boundary zone suppresses shear-driven sorting processes, and vertical mixing in the bulk of the current counterbalances kinetic sieving.

Mechanisms for this inferred mixing process might include turbulence, although this is unlikely, since interstitial fluid turbulence is suppressed at high particle concentration. More likely alternatives are that as unsteadiness develops and currents are forced to change thickness particle velocities become deflected from horizontal, which leads to mixing. Another possibility is that in polymict flow the local differences in pore pressure diffusion around large clasts enable localized changes in friction which instigate shear rotation, in a manner similar to Kelvin Helmholtz instability growth (Goldfarb, Glasser and Shinbrot, 2002; Rowley et al., 2011).

The experiments presented here clearly demonstrate that grainsize sorting is effectively achieved in dense granular currents, suggesting that either [1] good grainsize mixing in dense granular currents is not widespread, [2] that the scaling of the flume experiments is unable to capture behaviors observed within larger magnitude natural currents, or that [3] the sidewall observations in classic granular flume experiments are not representative of what might be happening within the rest of the current. Flume experiments have been unable to capture progressive aggradation of sediment from fluidized PDCs, with the current thickness being limited to hundreds rather than tens of thousands (or more) of particle diameters in natural currents. The pore pressure diffusion timescales are therefore faster in the laboratory, and friction at the base of the flow rapidly decelerates the entire package, rather than allowing sustained sedimentation and overpassing current simultaneously, leading to stepwise aggradation, as observed here. Similarly, experiments have clearly demonstrated

strong sidewall effects (Rowley et al., 2023) creating lateral velocity profiles equivalent in magnitude to the vertical velocity profiles (Smith et al., 2023). The laboratory conditions, therefore, are well suited to simulate currents which might form thin laminated and cross stratified packages, where reverse grading is often evident, but the highly efficient sorting we see here creates issues for the existing paradigm of mLT formation.

Careful work will be needed to explore this problem; the classic interpretation of mLT as an aggrading sample of the over-riding current either implies that the sorting mechanisms observed here are being suppressed, or that mLT is formed by some other process not captured here. It is possible that the scaling of the grainsize distribution to the thickness of the shearing layer may be important, or that the pore pressure in fluidized grainflows has a damping effect on granular segregation which we are losing through rapid pore pressure diffusion in upper course layers of our thin experimental currents. Interrogating the particle motions of fast moving fluidized granular currents has already granted us some insights to the velocity profiles at the sidewalls – achieving this for larger, more energetic currents, and interrogating currents away from the sidewall poses larger challenges.

6 Conclusions

Defluidising dense granular flows are spontaneously unsteady currents, even when provided with a steady and uniform sediment supply. At least some of this is likely a result of the velocity reduction in the head of the current as pore pressure reduces through time, and material in the current body is able to catch up. The creation of unsteady pulses within the currents can be seen as velocity and thickness fluctuations which must result in unsteady energy conditions closer to the bed. In addition, breaking waves and slushing at the free surface appear effective in transferring material into the dilute turbulent layer, which will enhance the transfer of fines from the dense layer beyond that achieved by elutriation alone.

Introducing diverse particle size distributions more akin to those observed in natural currents reveals complex behaviors with regard to both current and deposit structure, and begins to raise questions about some of our assumptions regarding the assembly of some ignimbrite stratigraphies. The extensive work to date on dense granular currents has focused almost exclusively on single or narrow (single-phi) particle size distributions. This work clearly demonstrates that sorting can occur in thin laminar granular flow in very short timescales, and as such there are many questions

remaining on what the impacts of this might be on fluidization and velocity profiles in these structured current layers.

There is clearly some mismatch between either how the laboratory simulations scale to mLT-depositing natural currents, or how we interpret the flow conditions which create this lithofacies in the field. It is possible, and even likely that some combination of both of these is true. If granular sorting is as effective in PDCs as we see here, then the interpretation of mLT as the deposit of a progressively aggrading dense granular layer requires the development of large-scale mixing processes within the dense current, with a large-scale vertical mixing rate which is greater than the sorting rate driven by granular temperature.

The presence or absence of mixing vs sorting processes has important implications for the application of numerical modelling. Critically, it implies that for currents where mixing is occurring, depth averaged numerical models such as VolcFlow (Kelfoun, 2017; Kelfoun et al., 2017; Gueugneau et al., 2024), IMEX2_SfloW2D (de' Michieli Vitturi et al., 2019) and TITAN2D (Patra et al., 2005; Charbonnier and Gertisser, 2009) may be even better suited to modelling dense layers than presumed. Mixing would be linked to relatively homogenous fluidization behaviors, pore pressure diffusion timescales, and therefore friction. While there will undoubtedly be considerable shear at the flow boundary zone, depth averaging would capture the largest portion of the current well, and as such can be considered powerful in reliably exploring flow mobility and risk potential in a robust manner. The extreme velocity profiles, and - as shown here - sorting profiles of thin laminar dense granular currents, however, make depth averaging more problematic. The vertical segregation of grainsizes, and resulting changes in pore pressure diffusion, and particle interactions would result in complex frictional changes which depth averaging is blind to.

Acknowledgments

This work compiles efforts from numerous projects over several years, which has in part been funded by a Université Blaise Pascal Postdoctoral Fellowship (PR), a British Society for Geomorphology Early Career Grant (PR), a Royal Society Award (IES\R2\222171) (RW), a University of Hull (Catastrophic Flows Research Cluster) PhD Scholarship (GS), and a EU Horizon 2020 Programme (Project GEOSTICK 712525)-funded University of Hull (Earth and Environment Institute) PhD Scholarship (NW).

Availability Statement

Data used in this publication are available at DOI: 10.5281/zenodo.8139271 under a Creative Commons Attribution 4.0 International license.

References

Andrews, B. J., & Manga, M. (2012). Experimental study of turbulence, sedimentation, and coignimbrite mass partitioning in dilute pyroclastic density currents. Journal of Volcanology and Geothermal Research, 225–226, 30–44. https://doi.org/10.1016/j.jvolgeores.2012.02.011

Bagnold, R. A. (1954). Experiments on a gravity-free dispersion of large solid spheres in a Newtonian fluid under shear. Proceedings of the Royal Society of London. Series A, Mathematical and Physical Sciences, 225(1160), 49–63.

Branney, M. J., & Kokelaar, B. P. (2002). Pyroclastic density currents and the sedimentation of ignimbrites. Geological Society.

Branney, M. J., & Kokelaar, P. (1997). Giant bed from a sustained catastrophic density current flowing over topography: Acatlán ignimbrite, Mexico. Geology, 25(2), 115–118. https://doi.org/10.1130/0091-7613(1997)025<0115:GBFASC>2.3.CO;2

Breard, E. C. P., Dufek, J., & Roche, O. (2019). Continuum Modeling of Pressure-Balanced and Fluidized Granular Flows in 2-D: Comparison With Glass Bead Experiments and Implications for Concentrated Pyroclastic Density Currents. Journal of Geophysical Research: Solid Earth, 124(6), 5557–5583. https://doi.org/10.1029/2018JB016874

Breard, E. C. P., Jones, J. R., Fullard, L., Lube, G., Davies, C., & Dufek, J. (2019). The Permeability of Volcanic Mixtures—Implications for Pyroclastic Currents. Journal of Geophysical Research: Solid Earth, 124(2), 1343–1360. https://doi.org/10.1029/2018JB016544

Breard, E. C. P., & Lube, G. (2017). Inside pyroclastic density currents – uncovering the enigmatic flow structure and transport behaviour in large-scale experiments. Earth and Planetary Science Letters, 458, 22–36. https://doi.org/10.1016/j.epsl.2016.10.016

Breard, E. C. P., Lube, G., Jones, J. R., Dufek, J., Cronin, S. J., Valentine, G. A., & Moebis, A. (2016). Coupling of turbulent and non-turbulent flow regimes within pyroclastic density currents. Nature Geoscience, 9(10), 767–771. https://doi.org/10.1038/ngeo2794

Brown, R. J., & Branney, M. J. (2004). Event-stratigraphy of a caldera-forming ignimbrite eruption on Tenerife: The 273 ka Poris Formation. Bulletin of Volcanology, 66(5), 392–416. https://doi.org/10.1007/s00445-003-0321-y

Brown, S. K., Jenkins, S. F., Sparks, R. S. J., Odbert, H., & Auker, M. R. (2017). Volcanic fatalities database: Analysis of volcanic threat with distance and victim classification. Journal of Applied Volcanology, 6(1). https://doi.org/10.1186/s13617-017-0067-4

Bursik, M. I., & Woods, A. W. (1996). The dynamics and thermodynamics of large ash flows. Bulletin of Volcanology, 58(2–3), 175–193. https://doi.org/10.1007/s004450050134

Calder, E. S., Sparks, R. S. J., & Gardeweg, M. C. (2000). Erosion, transport and segregation of pumice and lithic clasts in pyroclastic flows inferred from ignimbrite at Lascar Volcano, Chile.

Journal of Volcanology and Geothermal Research, 104(1–4), 201–235. https://doi.org/10.1016/S0377-0273(00)00207-9

Charbonnier, S. J., & Gertisser, R. (2009). Numerical simulations of block-and-ash flows using the Titan2D flow model: Examples from the 2006 eruption of Merapi Volcano, Java, Indonesia. Bulletin of Volcanology, 71(8), 953–959. https://doi.org/10.1007/s00445-009-0299-1

Chedeville, C., & Roche, O. (2014). Autofluidization of pyroclastic flows propagating on rough substrates as shown by laboratory experiments. Journal of Geophysical Research: Solid Earth, 119(3), 1764–1776. https://doi.org/10.1002/2013JB010554

Cole, P. D., Barclay, J., Robertson, R. E. A., Mitchell, S., Davies, B. V., Constantinescu, R., Sparks, R. S. J., Aspinall, W., & Stinton, A. (2024). Explosive sequence of La Soufrière, St Vincent, April 2021: Insights into drivers and consequences via eruptive products. Geological Society, London, Special Publications, 539(1), SP539-2022–2292. https://doi.org/10.1144/SP539-2022-292

de' Michieli Vitturi, M., Esposti Ongaro, T., Lari, G., & Aravena, A. (2019). IMEX_SfloW2D 1.0: A depth-averaged numerical flow model for pyroclastic avalanches. Geoscientific Model Development, 12(1), 581–595. https://doi.org/10.5194/gmd-12-581-2019

Dellino, P., Büttner, R., Dioguardi, F., Doronzo, D. M., La Volpe, L., Mele, D., Sonder, I., Sulpizio, R., & Zimanowski, B. (2010). Experimental evidence links volcanic particle characteristics to pyroclastic flow hazard. Earth and Planetary Science Letters, 295(1–2), 314–320. https://doi.org/10.1016/j.epsl.2010.04.022

Dellino, P., Dioguardi, F., Rinaldi, A., Sulpizio, R., & Mele, D. (2021). Inverting sediment bedforms for evaluating the hazard of dilute pyroclastic density currents in the field. Scientific Reports, 11(1), 21024. https://doi.org/10.1038/s41598-021-00395-3

Dellino, P., Zimanowski, B., Büttner, R., La Volpe, L., Mele, D., & Sulpizio, R. (2007). Large-scale experiments on the mechanics of pyroclastic flows: Design, engineering, and first results. Journal of Geophysical Research: Solid Earth, 112(4), 1–13. https://doi.org/10.1029/2006JB004313

Denlinger, R. P., & Iverson, R. M. (2001). Flow of variably fluidized granular masses across three-dimensional terrain: 2. Numerical predictions and experimental tests. Journal of Geophysical Research: Solid Earth, 106(B1), 553–566. https://doi.org/10.1029/2000jb900330

Doronzo, D. M. (2012). Two new end members of pyroclastic density currents: Forced convection-dominated and inertia-dominated. Journal of Volcanology and Geothermal Research, 219–220, 87–91. https://doi.org/10.1016/j.jvolgeores.2012.01.010

Douillet, G. A., Bernard, B., Bouysson, M., Chaffaut, Q., Dingwell, D. B., Gegg, L., Hoelscher, I., Kueppers, U., Mato, C., Ritz, V. A., Schlunegger, F., & Witting, P. (2019). Pyroclastic dune bedforms: Macroscale structures and lateral variations. Examples from the 2006 pyroclastic currents at Tungurahua (Ecuador). Sedimentology, 66(5), 1531–1559. https://doi.org/10.1111/sed.12542

Doyle, E. E., Hogg, A. J., & Mader, H. M. (2010). A two-layer approach to modelling the transformation of dilute pyroclastic currents into dense pyroclastic flows. Proceedings of the Royal Society A: Mathematical, Physical and Engineering Sciences, 467(2129), 1348–1371. https://doi.org/10.1098/rspa.2010.0402

Fries, A., Roche, O., & Carazzo, G. (2021). Granular mixture deflation and generation of pore fluid pressure at the impact zone of a pyroclastic fountain: Experimental insights. Journal of Volcanology and Geothermal Research, 414, 107226. https://doi.org/10.1016/j.jvolgeores.2021.107226

Geldart, D. (1973). Types of gas fluidization. Powder Technology, 7(5), 285–292. https://doi.org/10.1016/0032-5910(73)80037-3

Gilbertson, M. A. (2019). Estimation of the minimum fluidisation velocities in well-mixed bi-disperse fluidised beds. Powder Technology, 346, 433–440. https://doi.org/10.1016/j.powtec.2019.02.019

Gilbertson, M. A., & Eames, I. (2003). The influence of particle size on the flow of fluidised powders. Powder Technology, 131(2–3), 197–205. https://doi.org/10.1016/S0032-5910(02)00343-1

Giordano, G., De Benedetti, A. A., Diana, A., Diano, G., Esposito, A., Fabbri, M., Gaudioso, F., Marasco, F., Mazzini, I., Miceli, M., & others. (2010). Stratigraphy, volcano tectonics and evolution of the Colli Albani volcanic field. In The Colli Albani Volcano (pp. 43–97). Geological Society of London.

Girolami, L., Roche, O., Druitt, T. H., & Corpetti, T. (2010). Particle velocity fields and depositional processes in laboratory ash flows, with implications for the sedimentation of dense pyroclastic flows. Bulletin of Volcanology, 72(6), 747–759. https://doi.org/10.1007/s00445-010-0356-9

Goldfarb, D. J., Glasser, B. J., & Shinbrot, T. (2002). Shear instabilities in granular flows. Nature, 415(6869), 302–305. https://doi.org/10.1038/415302a

Gueugneau, V., Charbonnier, S., Miller, V. L., Cole, P., Grandin, R., & Dualeh, E. W. (2024). Modelling pyroclastic density currents of the April 2021 La Soufrière St. Vincent eruption: From rapid invasion maps to field-constrained numerical simulations. Geological Society, London, Special Publications, 539(1), SP539-2022–2290. https://doi.org/10.1144/SP539-2022-290

Gueugneau, V., Charbonnier, S., & Roche, O. (2022). PyroCLAST: A new experimental framework to investigate overspilling of channelized, concentrated pyroclastic currents. Bulletin of Volcanology, 85(1), 5. https://doi.org/10.1007/s00445-022-01623-y

Houghton, B. F., Wilson, C. J. N., Fierstein, J., & Hildreth, W. (2004). Complex proximal deposition during the Plinian eruptions of 1912 at Novarupta, Alaska. Bulletin of Volcanology, 66(2), 95–133. https://doi.org/10.1007/s00445-003-0297-7

Israel, R., & Rosner, D. E. (1982). Use of a Generalized Stokes Number to Determine the Aerodynamic Capture Efficiency of Non-Stokesian Particles from a Compressible Gas Flow. Aerosol Science and Technology, 2(1), 45–51. https://doi.org/10.1080/02786828308958612

Iverson, R. M. (1997). The physics of debris flows. Reviews of Geophysics, 35(3), 245–296. https://doi.org/10.1029/97RG00426

Kelfoun, K. (2017). A two-layer depth-averaged model for both the dilute and the concentrated parts of pyroclastic currents. Journal of Geophysical Research: Solid Earth, 122(6), 4293–4311. https://doi.org/10.1002/2017JB014013

Kelfoun, K., Gueugneau, V., Komorowski, J.-C., Aisyah, N., Cholik, N., & Merciecca, C. (2017). Simulation of block-and-ash flows and ash-cloud surges of the 2010 eruption of Merapi volcano with a two-layer model. Journal of Geophysical Research: Solid Earth, 122(6), 4277–4292. https://doi.org/10.1002/2017JB013981

Lube, G., Breard, E. C. P., Esposti-Ongaro, T., Dufek, J., & Brand, B. (2020). Multiphase flow behaviour and hazard prediction of pyroclastic density currents. Nature Reviews Earth and Environment, 1(7), 348–365. https://doi.org/10.1038/s43017-020-0064-8

Lube, G., Breard, E. C. P., Jones, J., Fullard, L., Dufek, J., Cronin, S. J., & Wang, T. (2019). Generation of air lubrication within pyroclastic density currents. Nature Geoscience, 12(5), 381–386. https://doi.org/10.1038/s41561-019-0338-2

Lube, G., Cronin, S. J., Platz, T., Freundt, A., Procter, J. N., Henderson, C., & Sheridan, M. F. (2007). Flow and deposition of pyroclastic granular flows: A type example from the 1975 Ngauruhoe eruption, New Zealand. Journal of Volcanology and Geothermal Research, 161(3), 165–186. https://doi.org/10.1016/j.jvolgeores.2006.12.003

Meruane, C., Tamburrino, A., & Roche, O. (2012). Dynamics of dense granular flows of small-and-large-grain mixtures in an ambient fluid. Physical Review E - Statistical, Nonlinear, and Soft Matter Physics, 86(2), 1–13. https://doi.org/10.1103/PhysRevE.86.026311

Ort, M. H., Orsi, G., Pappalardo, L., & Fisher, R. V. (2003). Anisotropy of magnetic susceptibility studies of depositional processes in the Campanian Ignimbrite, Italy. Bulletin of Volcanology, 65(1), 55–72. https://doi.org/10.1007/s00445-002-0241-2

Patra, A. K., Bauer, A. C., Nichita, C. C., Pitman, E. B., Sheridan, M. F., Bursik, M., Rupp, B., Webber, A., Stinton, A. J., Namikawa, L. M., & Renschler, C. S. (2005). Parallel adaptive numerical simulation of dry avalanches over natural terrain. Journal of Volcanology and Geothermal Research, 139(1–2), 1–21. https://doi.org/10.1016/j.jvolgeores.2004.06.014

Pollock, N. M., Brand, B. D., Rowley, P. J., Sarocchi, D., & Sulpizio, R. (2019). Inferring pyroclastic density current flow conditions using syn-depositional sedimentary structures. Bulletin of Volcanology, 81(8). https://doi.org/10.1007/s00445-019-1303-z

Roche, O. (2012). Depositional processes and gas pore pressure in pyroclastic flows: An experimental perspective. Bulletin of Volcanology, 74(8), 1807–1820. https://doi.org/10.1007/s00445-012-0639-4

Roche, O., Gilbertson, M. A., Phillips, J. C., & Sparks, S. S. J. (2004). Experimental study of gas-fluidized granular flows with implications for pyroclastic flow emplacement. Journal of Geophysical Research: Solid Earth, 109(10), 1–14. https://doi.org/10.1029/2003JB002916

Rowley, P., Giordano, G., Silleni, A., Smith, G., Trolese, M., & Williams, R. (2023). Stationary surface waves and antidunes in dense pyroclastic density currents [Preprint]. Earth ArXiv. https://doi.org/10.31223/X5TW8V

Rowley, P. J., Kokelaar, P., Menzies, M., & Waltham, D. (2011). Shear-derived mixing in dense granular flows. Journal of Sedimentary Research, 81(12). https://doi.org/10.2110/jsr.2011.72

Rowley, P. J., Roche, O., Druitt, T. H., & Cas, R. (2014). Experimental study of dense pyroclastic density currents using sustained, gas-fluidized granular flows. Bulletin of Volcanology, 76(9). https://doi.org/10.1007/s00445-014-0855-1

Savage, S. B., & Hutter, K. (1991). The dynamics of avalanches of granular materials from initiation to runout. Part I: Analysis. Acta Mechanica, 86(1), 201–223. https://doi.org/10.1007/BF01175958

Scarpati, C., Cole, P., & Perrotta, A. (1993). The Neapolitan Yellow Tuff—A large volume multiphase eruption from Campi Flegrei, Southern Italy. Bulletin of Volcanology, 55(5), 343–356. https://doi.org/10.1007/BF00301145

Smith, G. M., Williams, R., Rowley, P. J., & Parsons, D. R. (2018). Investigation of variable aeration of monodisperse mixtures: Implications for pyroclastic density currents. Bulletin of Volcanology, 80(8). https://doi.org/10.1007/s00445-018-1241-1

Smith, G., Rowley, P., Williams, R., Giordano, G., Trolese, M., Silleni, A., Parsons, D. R., & Capon, S. (2020). A bedform phase diagram for dense granular currents. Nature Communications, 11(1). https://doi.org/10.1038/s41467-020-16657-z

Smith, G., Williams, R., Rowley, P., & Parsons, D. (2023). Characterising the flow-boundary zone in fluidised granular currents [Preprint]. EarthArXiv. https://doi.org/10.31223/X56958

Smith, N. J., & Kokelaar, B. P. (2013). Proximal record of the 273 ka Poris caldera-forming eruption, Las Cañadas, Tenerife. Bulletin of Volcanology, 75(11), 1–21. https://doi.org/10.1007/s00445-013-0768-4

Sulpizio, R., & Dellino, P. (2008). Sedimentology, Depositional Mechanisms and Pulsating Behaviour of Pyroclastic Density Currents. In Developments in Volcanology (Vol. 10, pp. 57–96). Elsevier. https://doi.org/10.1016/S1871-644X(07)00002-2

Sulpizio, R., Dellino, P., Doronzo, D. M., & Sarocchi, D. (2014). Pyroclastic density currents: State of the art and perspectives. Journal of Volcanology and Geothermal Research, 283, 36–65. https://doi.org/10.1016/j.jvolgeores.2014.06.014

Valentine, G. A., Palladino, D. M., DiemKaye, K., & Fletcher, C. (2019). Lithic-rich and lithic-poor ignimbrites and their basal deposits: Sovana and Sorano formations (Latera caldera, Italy). Bulletin of Volcanology, 81(4), 29. https://doi.org/10.1007/s00445-019-1288-7

Walker, G. P. L. (1981). Generation and dispersal of fine ash and dust by volcanic eruptions. Journal of Volcanology and Geothermal Research, 11(1), 81–92. https://doi.org/10.1016/0377-0273(81)90077-9

Zhou, W., Lai, Z., Ma, G., Yang, L., & Chen, Y. (2016). Effect of base roughness on size segregation in dry granular flows. Granular Matter, 18(4), 83. https://doi.org/10.1007/s10035-016-0680-7

Zrelak, P. J., Pollock, N. M., Brand, B. D., Sarocchi, D., & Hawkins, T. (2020). Decoding pyroclastic density current flow direction and shear conditions in the flow boundary zone via particle-fabric analysis. Journal of Volcanology and Geothermal Research, 402, 106978. https://doi.org/10.1016/j.jvolgeores.2020.106978